Int. J. Environ. Sci. Technol. (2015) 12:2447–2454
DOI 10.1007/s13762-014-0681-1

ORIGINAL PAPER

Water displacement by surfactant solution: an experimental study to represent wastewater loss from sewers to saturated soil

M. Nikpay · D. Lazik · P. Krebs

Received: 27 May 2014 / Revised: 29 August 2014 / Accepted: 7 October 2014 / Published online: 19 October 2014

Abstract Leakage of wastewater from sewer lines may result in contamination of soil and groundwater. Our investigation dealt with the effects of surfactant as one of the constituents of wastewater on the infiltration process of wastewater through soil. To that aim, in a laboratory experiment, a column was uniformly packed with glass beads of 0.25–0.50 mm diameter and equipped with sensors to measure local fluid pressure at three observation points along the direction of flow. The artificial laboratory wastewater was created by adding a commercially available detergent to degassed tap water producing surfactant concentrations between 8 and 16 mg l^{-1}. The displacement process of degassed tap water by such a particle-free artificial wastewater was studied by loading the surfactant solution into the saturated glass beads column. Short-term pressure changes were observed while the interface between water and surfactant solution passed the observation points within the column. The pressure peaks increased for higher surfactant concentrations. The theory of growing interface between surfactant solution and clean water by aggregation of monomers to a double layer could be supported by the column experiments.

Keywords Wastewater exfiltration · Interface · Sewer · Interfacial tension

M. Nikpay (✉) · P. Krebs
Institute for Urban Water Management, TU Dresden,
01062 Dresden, Germany
e-mail: nikpay11@gmail.com

D. Lazik
Department Soil Physics, Helmholtz Centre for Environmental Research – UFZ, Theodor-Lieser-Str. 4, 06120 Halle, Germany

Introduction

Sanitary systems are considered as one of the most important hygienic structures in urban areas. From leaky sewer systems, wastewater conceivably lost and infiltrates into the soil and eventually into ground water that can seriously affect water resources quality (Ellis et al. 2009; Karpf et al. 2011; Schwarzenbach et al. 2006; Wolf et al. 2006). From the sewer point of view, this process is known as exfiltration. In this respect, various studies identified a sealing or colmation zone varying between 10 to 50 mm is decreasing the exfiltration (Ellis et al. 2010; Rutsch et al. 2008). Although considerable work has been done on the infiltration process of wastewater to the soil–water system, there is insufficient quantifiable evidence to determine how such leakage is controlled by the colmation zone due to the complexity and nature of the sewage and its components.

Detergents containing surfactants are known for their highest concentrations of organic chemicals found in wastewater (Field et al. 1992; Shafran et al. 2005). The studies on grey-water infiltration into the soil confirmed that surfactants can potentially enhance changes to the soil structures, e.g. soil hydrophobicity (Travis et al. 2010). These characteristics associated with surfactants emphasising the importance of fundamental investigations in the hydro-physical properties of the soil (Abu-Zreig et al. 2003). In addition, the problem of measuring interfacial tension in porous media is related to the geometric factors, e.g. interfacial area defined in macro-scale description while there is no clarity in micro-scale. Thus, it is important that the definition in macro-scale is consist with the micro-scale complement based on measurements correctly interpreted (Gray and Schrefler 2001).

The infiltrated wastewater into the saturated soil results in a multi-phase system that is characterised by fluid–fluid as well as by fluid–solid interfaces. Focusing only on fluid–fluid system, at a static liquid–liquid interface, the adsorption of surfactant molecules will develop an interfacial layer with a finite thickness based on the size of the adsorbed molecules. As Myers (2006) concluded, this adsorption may also alter the nature of the molecules of liquid phases located near the interface and result in an interfacial region larger than the surfactants molecular layer.

In a dynamic interface (i.e. moving interface through the column in our experiment), the adsorbed surfactants are expanding or contracting with the bulk liquid while being transported through varying cross-sectional widths and continuously re-establishing an electrostatic equilibrium. Hence, the surfactants molecular structure and their electrostatic charge play an important role as the transport mechanism to the interface. The rate of surfactant adsorption at interface is controlled by the transportation step of monomers to the near-interface region. This is basically driven by molecular diffusion (Macleod and Radke 1993) additionally then from the near-interface region to the interface, electrostatic charge becomes dominant (Zhmud and Tiberg 2005).

In our experimental study, we are exploring the phenomena occurring when a surfactants solution, used as an artificial wastewater, is loaded onto a saturated porous media, which is represented by glass beads within a column. To that aim, the detection of the dynamic effect is achieved by pressure measurements to relate the expanding surfactant aggregation at fluid–fluid interface to interfacial tension and monomers concentration. The generated tension as a function of time is monitored by dynamic pressure measurements to reveal the surfactant accumulation at the interface. Consequently, we will discuss the results of the experiment based on the explanation of surfactant formation at the dynamic fluid–fluid interface.

Kinetic theory of surfactant monomers interfacial aggregation

The micro-scale property of the fluid–fluid interface is the basis to explain the mechanism of the surfactant film formation by monomeric aggregation. We suggest that surfactant monomers adsorbing at the interface with water form a thin layer that is established through a bilayer organisation of monomers. The surfactant monomers adsorb at the interface and create the first line. The second line is attached with an opposite orientation, i.e. tail to tail with the first line. The effect of gravity, capillarity or diffusion on such structure is obviously too weak to damage the insoluble bilayer. The ultra-thin layer at the interface formed by high monomers concentration gradient is inducing an interfacial tension.

Figure 1 shows the set-up of liquid–liquid interfacial region. The surfactant solution is the liquid phase α, and water is the liquid phase β. According to Gibbs thermodynamics equation (Gibbs 1948), liquids are separated by a thin interfacial layer. The so-called interfacial excess Γ

$$\Gamma = \frac{N_s}{A}$$

is the result of the Gibbs model, representing the specific number of surfactant monomers N_s per unit interface area A (in m^{-2} or in mol m^{-2}). The double layer structural formation of surfactant molecules at the interface with water is built with two thin interfacial excesses Γ_1 and Γ_2. The surfactant monomers with regular transmission repeatedly are displaced from Γ_1 to Γ_2 (Fig. 2). This displacement goes along with a change in orientation, such that the monomers are arranged "tail to tail" between Γ_1 and Γ_2.

In Fig. 1, it is shown that surfactant concentration for the surfactant liquid phase α is considered below the critical micelle concentration (CMC). The concentration of surfactant molecules in phase α will reach a maximum at interface Γ_1 what is stabilising and eventually extending the boundary.

Our primary assumptions to describe the system are steady-state and laminar flow, uniform conditions at the interface and that there is no surface deformation between the two liquid phases α and β. Surface deformation is inducing topological changes on the initially created interface, and thus, the adsorption of the surfactants molecules can be interrupted (Fischer et al. 2006; Hu 2008).

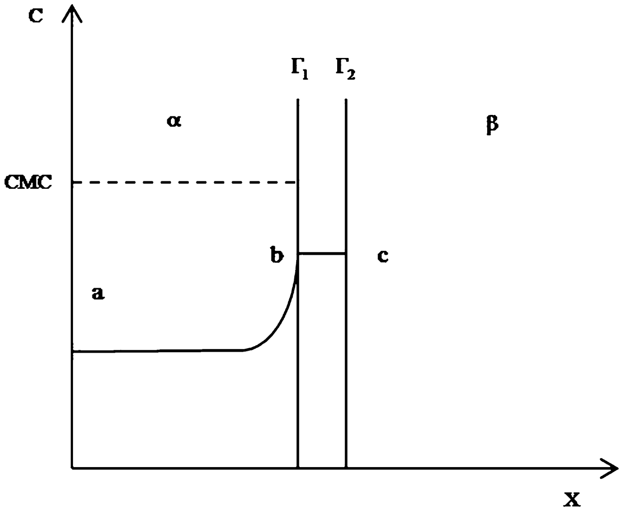

Fig. 1 Definition sketch of interface between the liquid phases α and β for surfactant solution and water, respectively. The interface between Γ_1 and Γ_2 separates two liquids. C is the concentration of surfactants in distance X. Two distinct kinematic regime *ab*–*bc* relates with the process of adsorption from surfactant solution at interface after injection at *a* to the background solution (water)

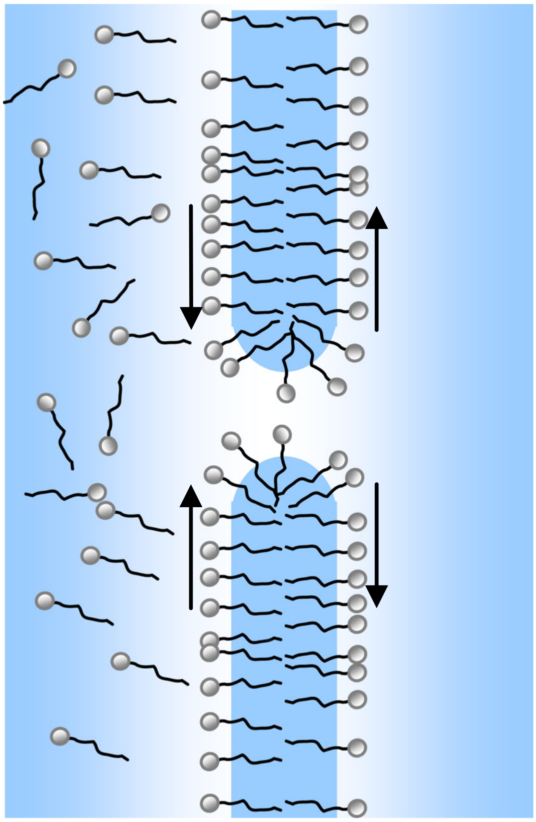

Fig. 2 Illustration of initial formation of thin surfactant film at the interface

The model is defined for time $0 \leq t \leq n$ in Γ_1 and Γ_2, where n represents the time when equilibrium concentration at Γ_1 and Γ_2 is reached. After reaching the equilibrium condition at $t \geq n$, it is hypothesised that no monomers are supplied from the bulk phase α to Γ_1.

Initially, at $t = 0$, the concentration at Γ_1 is equal to N_s/A, which represents an equilibrium state with the bulk concentration, while at Γ_2 $N_s/A = 0$. At time $0 < t < n$, the surfactant monomers are transferred to Γ_2. For the system reaching equilibrium concentration at time n after monomers were transferred from α to the interface, the concentrations at both Γ_1 and $\Gamma_2$will be equal to N_s/A (Fig. 1, b–c sector) at the end point of monomers transfer. Thus, the total number of monomers to cover the needs of the two-layer interface is doubled as compared to the initial condition at $t = 0$, while the specific surface density is the same at both layers Γ_1 and Γ_2, as this results from an equilibrium condition between the surfactants solution and the adjacent monomers interface layer. To fulfil this equilibrium condition, monomers must be supplied from the surfactants solution α to the interface Γ_1.

If the process continued at $n < t$, then the incorporation of the bulk phase α in the function of Γ_1 should be considered.

First option—for displacement of m monomers at Γ_1 to Γ_2—is that they will be replaced from bulk to $\Gamma_{1;}$ therefore, the equation reads $\Gamma_1 = N_s/A$, referring to steady state at Γ_1.

Second option—for displacement of m monomers at Γ_1–Γ_2—is that the bulk phase α will supply more than m monomers to Γ_1, indicating that the system has not yet reached a steady-state condition at Γ_1 and the monomers density at Γ_1 is still increasing towards a steady-state level.

The graph in Fig. 1 shows an increase in the concentration Γ_2 at $0 \leq t \leq n$ when the maximum concentration is equal to molecular surfactant concentration, C_{mol}. The total surfactant concentration below the CMC is equal to the local molecular surfactants concentration in the bulk solution and in the adsorbed interfaces (Starov 2004).

Materials and methods

Experimental set-up

We conducted column experiments in order to measure the dynamic interfacial tension in a saturated porous media as a result of surfactant adsorption at fluid–fluid interface. Figure 3 shows a sketch of the experimental apparatus used in this study. The test was performed within a metal column packed with glass beads with diameters ranging from 0.25 to 0.50 mm, which is close to the diameter of grains in the bedding layer of sewers. The column height was 296.8 mm with a cross-sectional area of 54.0 cm^2 (diameter 8.3 cm), and the glass beads package exhibited a porosity of 0.36. A pump was used to inject degassed water and surfactant solution from two different reservoirs while a three-way supply valve was applied before the column to change the flow direction from the reservoirs.

The flow rate was kept constant at 2.3 l h^{-1}. A commercial liquid detergent was used containing 20 % surfactants. Two concentrations of 8 and 16 mg l^{-1} of anionic surface active agent linear alkylbenzene sulphonic acid (LAS) were applied.

The LAS products are widely used as household detergents, dishwashing liquids and other domestic cleaners as well as in industrial applications such as emulsifiers. The concentration of anionic surfactant in grey water is reported to be between 0.7 and 44 mg l^{-1}, in domestic wastewater between 1 and 10 mg l^{-1} and for LAS products range from 3 to 21 mg l^{-1}(Henau et al. 1986; Adak et al. 2005). The critical micelle concentration (CMC) value for the surfactant used in the test is reported as 100 mg l^{-1}.

Degassed water produced from tap water is restored in the capped containers and used for preparing the solutions. Prior to each experiment, the porous media column was washed with water several times to ensure the removal of

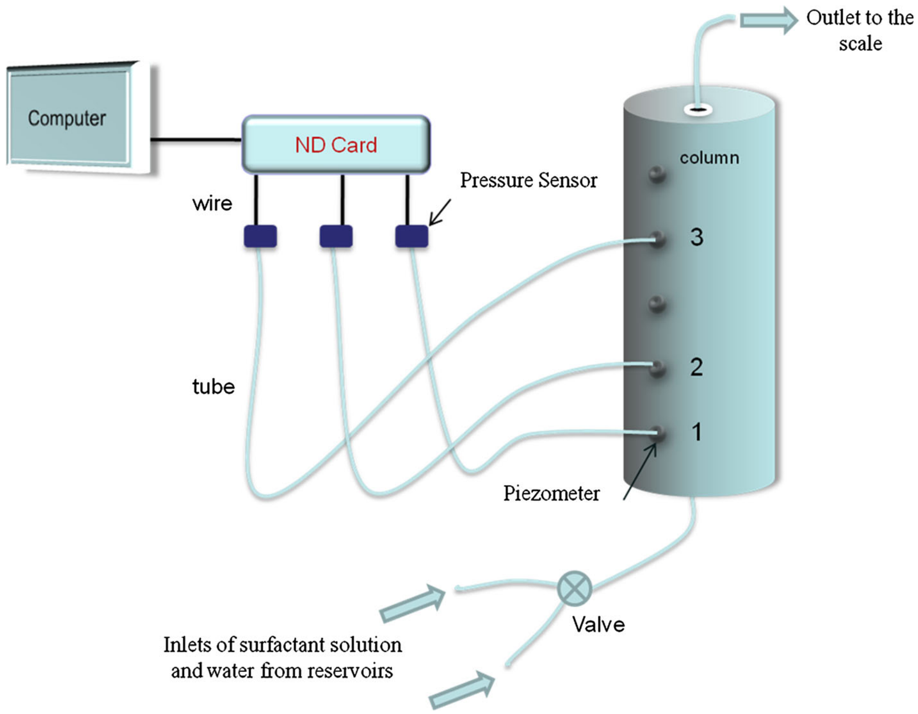

Fig. 3 Sketch of the column experiment and instrumental set-up

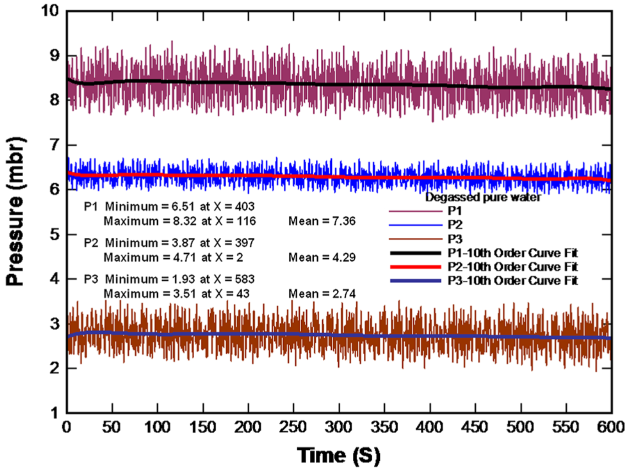

Fig. 4 Pressure variations at piezometer measurement points P1, P2 and P3 for pure tap water

any extraneous material. The sensors were calibrated by utilising artificial pressure developed within the connected tubes to ensure proper signals for each individual test. The flow in the test column was oriented vertically upward. Three pressure measurement points were used to measure the pressure changes during the passage of the flow along the column as shown in Fig. 3. The tubes were filled with water to avoid disturbing effects by gas bubbles. The column was saturated gently, and the outflow rate was measured continuously by an electronic scale. We regularly checked the signals on the monitor to assure constant pressure of the system before the surfactant solution was injected into the column (Fig. 4). This test was repeated several times to calibrate the system. The valve was opened gradually to omit any pressure wave propagation. Temperature was measured during the test and remained constant between 21 and 22 °C for both liquid reservoirs.

Instrumentation

The piezometer points are located in 5-cm steps and are connected via tubes to the pressure sensors. Measured data were continuously transmitted to the computer. Before the test, the piezometers were checked to omit any trapped gas inside the tubes.

In a capillary rise measuring method, the interfacial tension is defined as the work required to create a unit area of interface at a constant temperature, pressure and chemical potential. Since interfacial tension is always positive for interfaces between immiscible phases, it has a tendency to decrease the area of the interface inducing a curved interface with higher pressure on the convex than on the concave side of the interface (Drelich et al. 2002). The capillary pressure P_c between two fluids is explained by the Young–Laplace equation as:

$$P_{\mathrm{c}} = P_{\mathrm{nw}} - P_{\mathrm{w}} = \frac{2\sigma \ \cos\theta}{r}$$

where θ is a contact angle, σ is the surface tension between the wetting and non-wetting fluid phases, r is the radius of the interface curvature, P_{nw} is the pressure of the non-

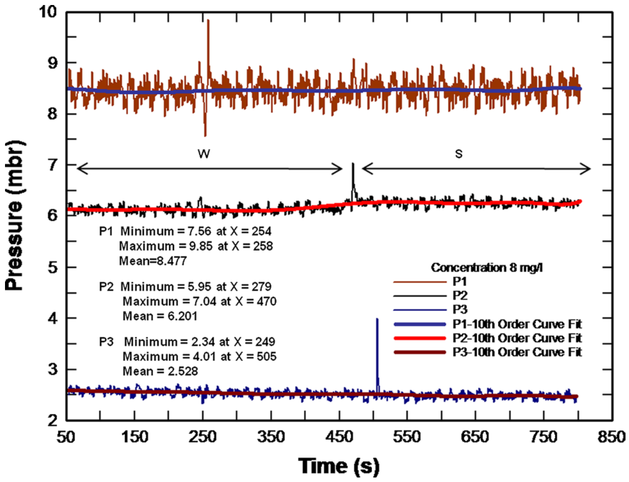

Fig. 5 Pressure variations at piezometer measurement points P1, P2 and P3 for surfactant concentration of 8 mg l^{-1}. W is representing water and S surfactant

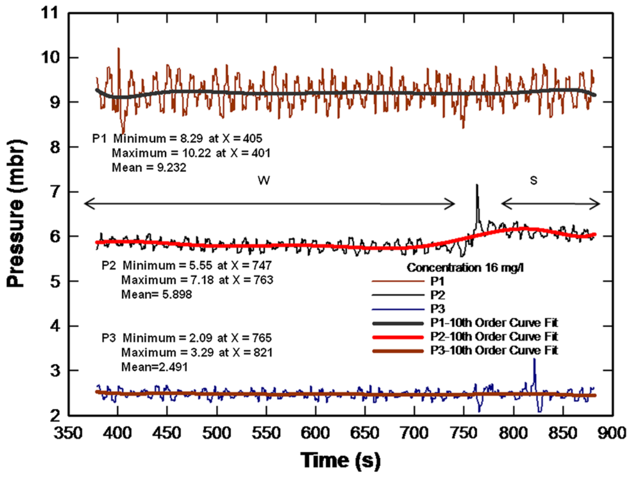

Fig. 6 Pressure variations at piezometer measurement points P1, P2 and P3 for surfactant concentration of 16 mg l^{-1}. W is representing water and S surfactant

wetting phase and P_w is the pressure of the wetting phase. Drelich et al. (2002) compared the accuracy and suitability of different techniques used in interfacial tension measurement and found that the capillary rise method exhibits a higher accuracy than other methods. Furthermore, the suitability of approach for measuring in surfactant solutions and two liquid systems was assessed to be good (Drelich et al. 2002). In our study, we measured the pressures P_{nw} and P_w on a piezometric basis.

The sensors were manufactured by SensorTechnics and equipped with a pressure range from 0 to a maximum of 2–5 Pa (20–50 mbar) at 25 °C. Each sensor is equipped with two pressure ports with inner diameters of 5 mm. They were connected to the data logger, NuDAM series model ND-6017, for analogue to digital conversion. The two portals of the sensor were used for pressure measurement at two locations. A digital weighing scale manufactured by Sartorius with a resolution of ± 0.01 g was connected to an ND card. Finally, the whole system was connected to a computer. Subsequently, the digitized values received by the computer are analysed using the software DASYLab (Zloto et al. 2012).

Results and discussion

Using the experimental set-up as described above, after calibration and flushing procedure, the tests were started with recording the pressure changes. As the liquid interface between tap water and surfactant solution was passing over the first piezometer point P1 (Figs. 5, 6), a peak was observed which after a few seconds decreased back to the initial bulk pressure variation range. Slightly later, a similar peak was measured in P2. These observations showed that the transit of the liquid interface was moving up with the flow direction and can be detected with a short pressure peak. After the peak in P2, the pressure slightly increased as compared to that before the peak (Figs. 5, 6). This effect is somewhat more distinct for the higher surfactant concentration of 16 mg l^{-1}, obviously indicating that the slight pressure increase is caused by the presence of surfactant.

The cause of pressure peak can be related to the aggregation of surfactant monomers forming a thin film at the interface of the fluids, inducing a signal when passing P1 and P2. More precisely, a meniscus is assumed to have been formed at the fluids interface due to interfacial tension (Joekar-Niasar et al. 2010; Held and Celia 2001). In the initial formation phase, in the capillary tubes with varying cross section, the meniscus was unstable. However, with propagation through the column, it became more stable. The surfactant layer at the interface was maintained along the column as surfactant monomers were transported from the bulk to the interface and thus increasing its stability. Consequently, the pressures of the fluids before and after the passage of the interface are to some extent decoupled.

The concentration of anionic surfactant applied in the test was below CMC. Hence, the concentration was in the monomeric concentration range. This concentration would not maintain the stability of the interface film for a long period beyond the experimental phase because the bulk liquid cannot supply enough monomers to satisfy the needs of the dynamic fluid–fluid interface, loosing monomers to the ambient fluid and to solids surfaces. However, as less energy is required for control at a liquid–liquid than at the liquid–solid (Birdi 2002), it can be concluded that

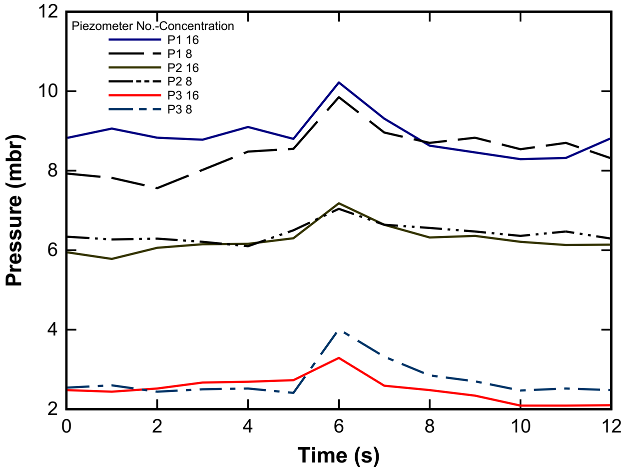

Fig. 7 Comparing pressure variations at piezometer measurement points P1, P2 and P3 for surfactant concentration of 8 and 16 mg l^{-1}

adsorption of surfactant monomers is primarily easier at fluid–fluid interface.

In Fig. 7, the pressure values in check points P1, P2 and P3 are compared for surfactant concentrations of 16 and 8 mg l^{-1} for a short time window around the interface peak. The graphs show higher pressure for the higher surfactant concentration after the peak at P2. In P1, this effect is not yet pronounced. Since surfactants tend to stabilize the fluids interface with higher molecular concentration, monomers accumulate behind the moving meniscus. This results in a decrease in the bulk surfactant concentration towards the moving meniscus (Starov 2004). Additionally, we assume that a bilayer of monomers at fluid–fluid interface is formed (see Fig. 2). Figure 7 shows that measurements in point P3 deviate from those in points P1 and P2 in as much as the pressure peak is significantly higher for the lower surfactant concentration of 8 mg l^{-1} than for 16 mg l^{-1}. This deviation from the expected effect may be the result of monomeric adsorption at the pores which is more pronounced for higher surfactants concentration, thereby increasing the hydrophobicity of the solids surface and reducing flow and peak capacity in preferential pathway (Wang et al. 2000). Subsequently, the push-out of water from a pore throat can be more pronounced for lower surfactant concentration after the water/surfactant solution interface was decelerating upstream of the throat, resulting in a "Haines Jump" (Reeves and Celia 1996).

The curvature of meniscus differs depending on the geometry condition, i.e. at the pore throat constriction or inside the pore throat. However, an average meniscus curvature might be acceptable for the whole system (Joekar-Niasar and Hassanizadeh 2011). The movement and formation of individual fluid–fluid interfaces at conduits is governed by the microscopic effects in the region of the meniscus (Reeves and Celia 1996).

Consequently, the pressure increase after passage of the fluid–fluid interface indicates an influence on the flow conditions through a slight increase of the pressure head as driving force and hence increasing the flow rate through the colmation layer.

Table 1 shows the average pressure values recorded 100 s before and after the passage of the pressure peak. If we assume that the pressure distribution in the column is in a steady-state condition before and after the peak, respectively, then we can expect the average value of the pressure before the aggregated surfactant layer to be the pressure of saturation. Comparing the results for surfactant concentration of 16 mg l^{-1} in P1, the average value is almost the same before and after the interface peak, what might indicate the low monomeric concentration after the interface passage. In the next check points, two phenomena are possible. First, the bulk is satisfying the needs for monomers of the mobile layer and resulting in increased pressure at P2. Secondly, there are not enough monomers in the bulk liquid and the pressure drops because of low monomeric concentration behind the interface. At check point P2 for 16 mg l^{-1}, a slight increase in the average pressure value after the peak is observed, while at check point P3 for 16 mg l^{-1}, the pressure returns approximately to the value measured before the peaks passage. Based on this data, we anticipate a decrease of the monomers concentration in the bulk after the film.

For surfactant concentration of 8 mg l^{-1}, the behaviour in P2 and P3 is similar as for 16 mg l^{-1}. At P1, unlike as for 16 mg l^{-1}, the average pressure value showed an increase after the peak. Obviously, the equilibrium condition is established more rapidly for lower surfactants concentration.

Table 1 Average pressure for 100 s before and after the peak value

	Piezometer No. 1		Piezometer No. 2		Piezometer No. 3	
	16 mg l^{-1}	8 mg l^{-1}	16 mg l^{-1}	8 mg l^{-1}	16 mg l^{-1}	8 mg l^{-1}
Average pressure (mbr) of 100 s before the peak value	9.214	8.418	5.798	6.166	2.49	2.508
Peak value (mbr)	10.22	9.85	7.18	7.04	3.29	4.01
Average pressure (mbr) of 100 s after the peak value	9.206	8.478	6.136	6.277	2.472	2.498

Conclusion

With regard to the exfiltration of wastewater from sewers into the soil, surfactants are an important group of wastewater constituents as their adsorption function at the interface to surfactant-free fluids and to the soil matrix changes is influencing the flow behaviour in porous media, especially that in the interfacial region.

In order to study these phenomena around the interface, we performed a column experiment using a surfactants solution loaded on a porous medium saturated with clean water. Pressure measurements at several points were carried out continuously and specifically during the passage of the interface between pure water and surfactant solution (i.e. groundwater displaced by exfiltrating sewage). The results show that the fluid pressure (peak) at the interface has a relationship with the surfactants concentration and supports the hypothesis a layer of aggregated surfactant monomers is generated at the interface associated with interfacial tension. With such an interface, the displacement of clean water by a surfactants solution is rigid and dominated by surface tension effects. Besides, the generated fluid pressure by this interface can increase the flow capacity through the colmation layer. It can thus be hypothesised that in soil around leaky sewers, processes especially in the colmation layer are to a large extent determined by the effects of surfactants. Further, the stable interface between pure water and surfactant solution indicates that mixture between the two liquids phases is weak. This meant that wastewater concentration is hardly diluted by groundwater around exfiltration leaks in sewers.

While the work presented here was focused on the fluid–fluid interface, further investigation has to be carried out on the interaction of surfactant solution with the porous matrix.

Acknowledgments The work was kindly supported by Helmholtz Interdisciplinary Graduate School for Environmental Research (HIGRADE).

References

Abu-Zreig M, Rudra R, Dickinson W (2003) Effect of application of surfactants on hydraulic properties of soils. Biosyst Eng 84(3):363–372

Adak A, Bandyopadhyay M, Pal A (2005) Removal of anionic surfactant from wastewater by alumina: a case study. Colloids Surf A: Physicochem Eng Asp 254(1):165–171

Birdi KS (2002) Self-assembly monolayer structures of lipids and macromolecules at interfaces. Kluwer Academic, New York

Drelich J, Fang Ch, White CL (2002) Measurement of interfacial tension in fluid-fluid systems. In: Hubbard AT (ed) Encyclopedia of surface and colloid science, vol 1. Marcel Dekker, Inc., Michigan Technological University, Houghton, pp 3158–3163

Ellis JB, Revitt DM, Vollertsen J, Blackwood DJ (2009) Sewer exfiltration and the colmation layer. Water Sci Technol 59(11):2273–2280

Ellis J, Revitt D, Karpf C, Krebs P (2010) The exfiltration process and the colmation layer. Assessing infiltration and exfiltration on the performance of urban sewer systems (APUSS), pp 61–70

Field J, Leenheer J, Thorn K, Barber L II, Rostad C, Macalady D, Daniel S (1992) Identification of persistent anionic surfactant-derived chemicals in sewage effluent and groundwater. J Contam Hydrol 9(1):55–78

Fischer P, Windhab EJ, Megias-Alguacil D (2006) Determination of the interfacial tension of low density difference liquid–liquid systems containing surfactants by droplet deformation methods. Chem Eng Sci 5:1386–1394

Gibbs JW (1948) The collected works of J. Willard Gibbs, 1st edn. Yale University Press, New Haven

Gray W, Schrefler B (2001) Thermodynamic approach to effective stress in partially saturated porous media. Eur J Mech-A Solids 20(4):521–538

Held R, Celia M (2001) Modeling support of functional relationships between capillary pressure, saturation, interfacial area and common lines. Adv Water Resour 24(3):325–343

Henau HD, Mathijs E, Hopping W (1986) Linear alkylbenzene sulfonates (LAS) in sewage sludges, soils and sediments: analytical determination and environmental safety considerations. Int J Environ Anal Chem 26(3–4):279–293

Hu Y (2008) Determination of interfacial tension between two immiscible polymers with and without surfactants at the interface. J Colloid Interface Sci 319(1):287–294

Joekar-Niasar V, Hassanizadeh SM (2011) Specific interfacial area: the missing state variable in two-phase flow equations? Water Resour Res 47(5). doi:10.1029/2010WR009291

Joekar-Niasar V, Hassanizadeh S, Dahle H (2010) Non-equilibrium effects in capillarity and interfacial area in two-phase flow: dynamic pore-network modelling. J Fluid Mech 655:38–71

Karpf C, Hoeft S, Scheffer C, Fuchs L, Krebs P (2011) Groundwater infiltration, surface water inflow and sewerage exfiltration considering hydrodynamic conditions in sewer systems. Water Sci Technol 63(9):1841–1848

Macleod C, Radke C (1993) A growing drop technique for measuring dynamic interfacial tension. J Colloid Interface Sci 160(2):435–448

Myers D (2006) Surfactant science and technology, 3rd edn. Wiley-Interscience, New Jersey

Reeves PC, Celia MA (1996) A functional relationship between capillary pressure, saturation, and interfacial area as revealed by a pore-scale network model. Water Resour Res 32(8):2345–2358

Rutsch M, Rieckermann J, Cullmann J, Ellis J, Vollertsen J, Krebs P (2008) Towards a better understanding of sewer exfiltration. Water Res 42(10):2385–2394

Schwarzenbach R, Escher B, Fenner K, Hofstetter T, Johnson C, Von Gunten U, Wehrli B (2006) The challenge of micropollutants in aquatic systems. Science 313(5790):1072–1077

Shafran A, Gross A, Ronen Z, Weisbrod N, Adar E (2005) Effects of surfactants originating from reuse of greywater on capillary rise in the soil. Water Sci Technol 52(10):57–166

Starov V (2004) Surfactant solutions and porous substrates: spreading and imbibition. Adv Colloid Interface Sci 111(1):3–27

Travis M, Wiel-Shafran A, Weisbrod N, Adar E, Gross A (2010) Greywater reuse for irrigation: effect on soil properties. Sci Total Environ 408(12):2501–2508

Wang Z, Wu Q, Wu L, Ritsema C, Dekker L, Feyen J (2000) Effects of soil water repellency on infiltration rate and flow instability. J Hydrol 231:265–276

Wolf L, Eiswirth M, Hoetzl H (2006) Assessing sewer–groundwater interaction at the city scale based on individual sewer defects and marker species distributions. Environ Geol 49(6):849–857

Zhmud B, Tiberg F (2005) Interfacial dynamics and structure of surfactant layers. Adv Colloid Interface Sci 113(1):21–42

Zloto T, Ptak P, Prauzner T (2012) Analysis of signals from inductive sensors by means of the DasyLab software. Annal UMCS Inform 12(1):31–37